Supplementary Materials
for

Synthesis, structural and magnetic properties of cobalt(II) complexes with pyridine-based macrocyclic ligand containing two pyridine pendant arms

Eva Zahradníková,[a] Céline Pichon,[b] Carine Duhayon,[b] Jean-Pascal Sutter,[b*] Petr Halaš,[a] and Bohuslav Drahoš[a*]

[a] *Department of Inorganic Chemistry, Faculty of Science, Palacký University, 17. listopadu 12, CZ-771 46 Olomouc, Czech Republic, Fax: +420 585 634 954. Tel: +420 585 634 429. E-mail: bohuslav.drahos@upol.cz*
[b] *Laboratoire de Chimie de Coordination du CNRS (LCC-CNRS), Université de Toulouse, CNRS, Toulouse, France. E-mail : jean-pascal.sutter@lcc-toulouse.fr*

Table of content:

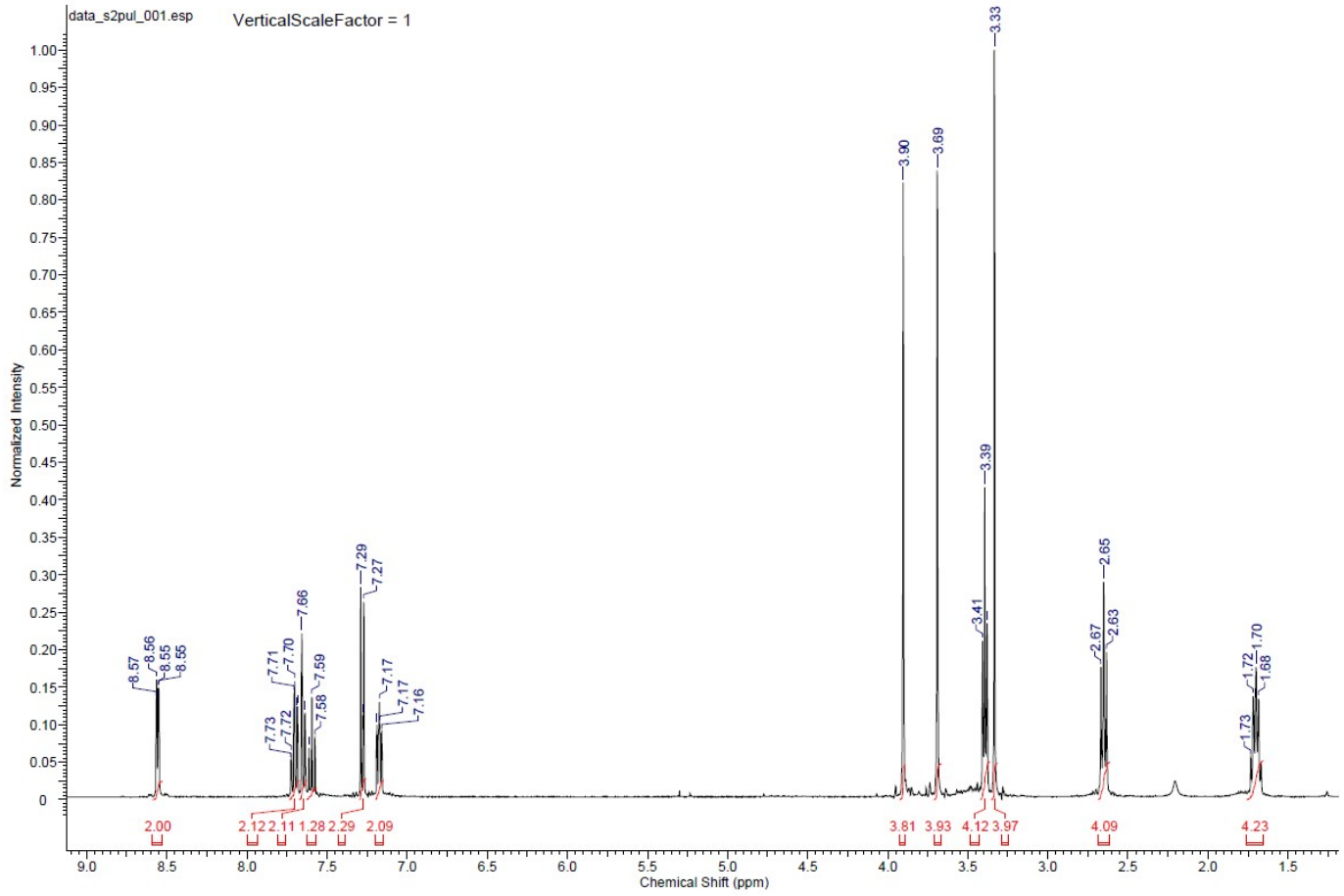

Figure S1: ^{1}H NMR spectrum (400 MHz, $CDCl_3$) of **L** (3,14-bis(2-methylpyridine)-3,14,20-triaza-7,10-dioxabicyclo[14.3.1]dodeca-1(20),16,18-triene) with a residual peak of $CHCl_3$ at 7.27 ppm (^{1}H).

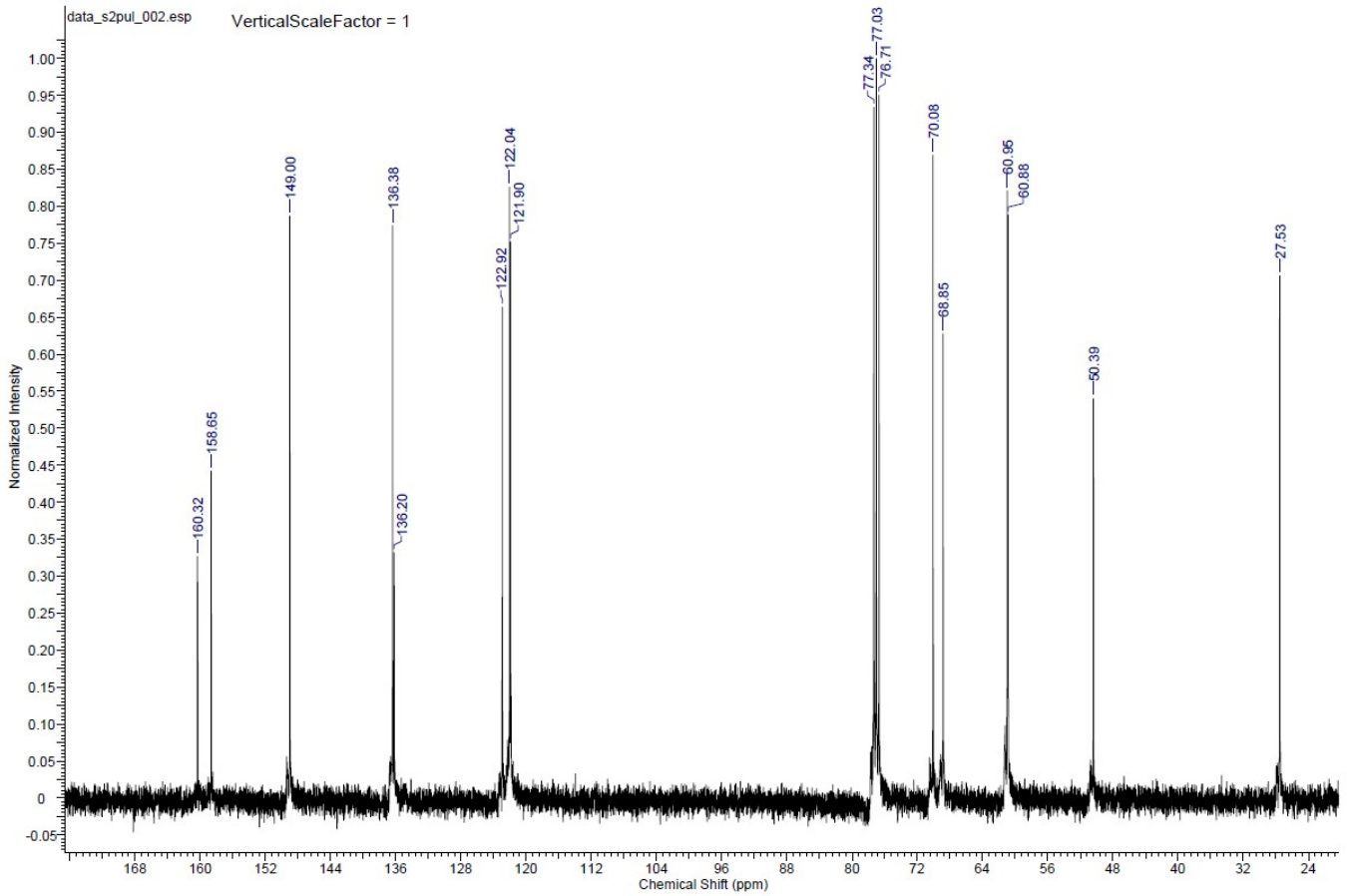

Figure S2: ^{13}C NMR spectrum (400 MHz, $CDCl_3$) of **L** (3,14-bis(2-methylpyridine)-3,14,20-triaza-7,10-dioxabicyclo[14.3.1]dodeca-1(20),16,18-triene) with a residual peak of $CHCl_3$ at 77.0 ppm (^{13}C).

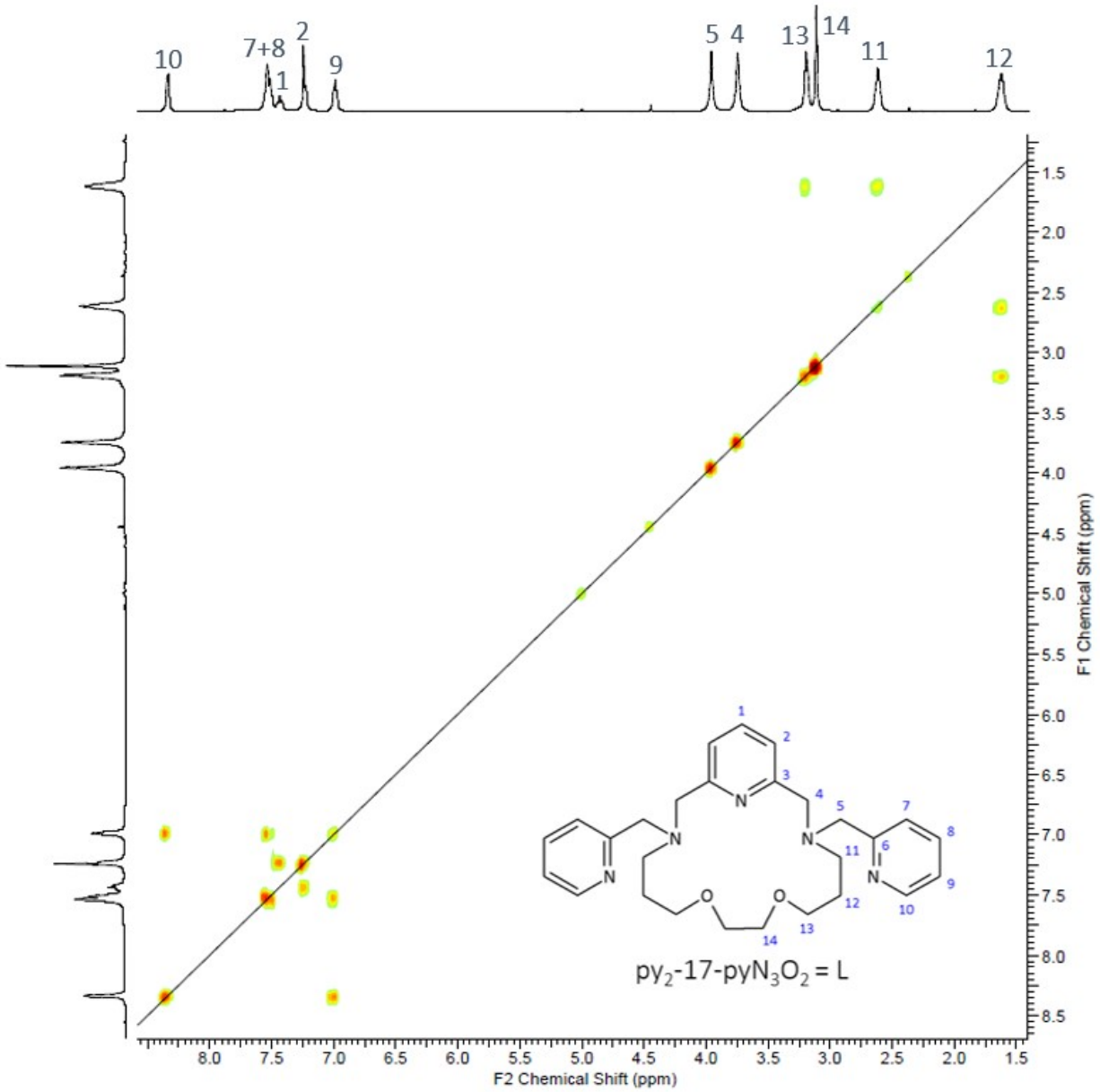

Figure S3: ^{1}H–^{1}H gs-COSY NMR spectrum (400 MHz, $CDCl_3$) of **L** (3,14-bis(2-methylpyridine)-3,14,20-triaza-7,10-dioxabicyclo[14.3.1]dodeca-1(20),16,18-triene) with a residual peak of $CHCl_3$ at 7.27 ppm (^{1}H).

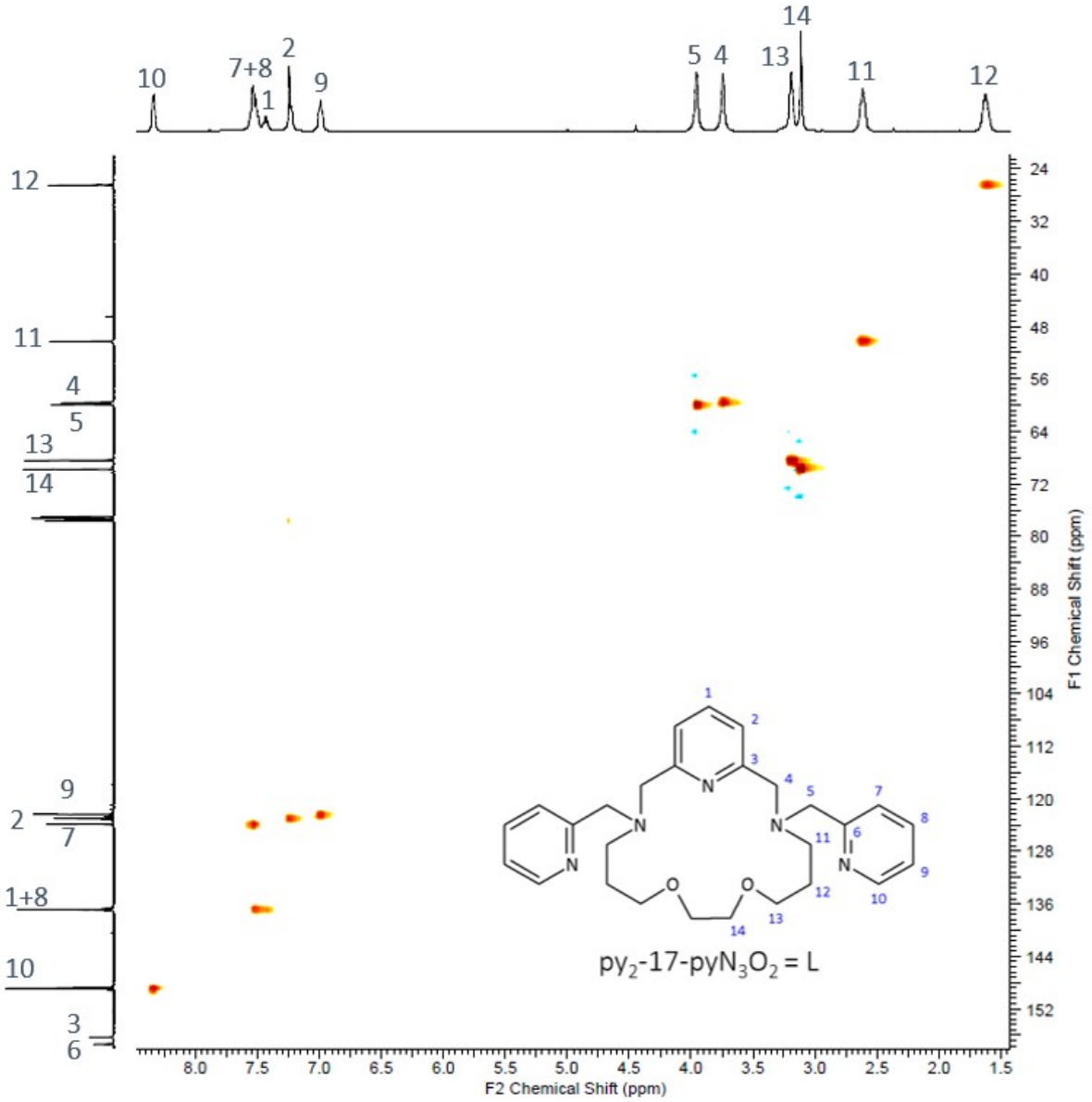

Figure S4: ^{1}H–^{13}C *gs*-HMQC NMR spectrum (400 MHz, $CDCl_3$) of **L** (3,14-bis(2-methylpyridine)-3,14,20-triaza-7,10-dioxabicyclo[14.3.1]dodeca-1(20),16,18-triene) with a residual peak of $CHCl_3$ at 7.27 ppm (^{1}H) and $CDCl_3$ at 77.0 ppm (^{13}C).

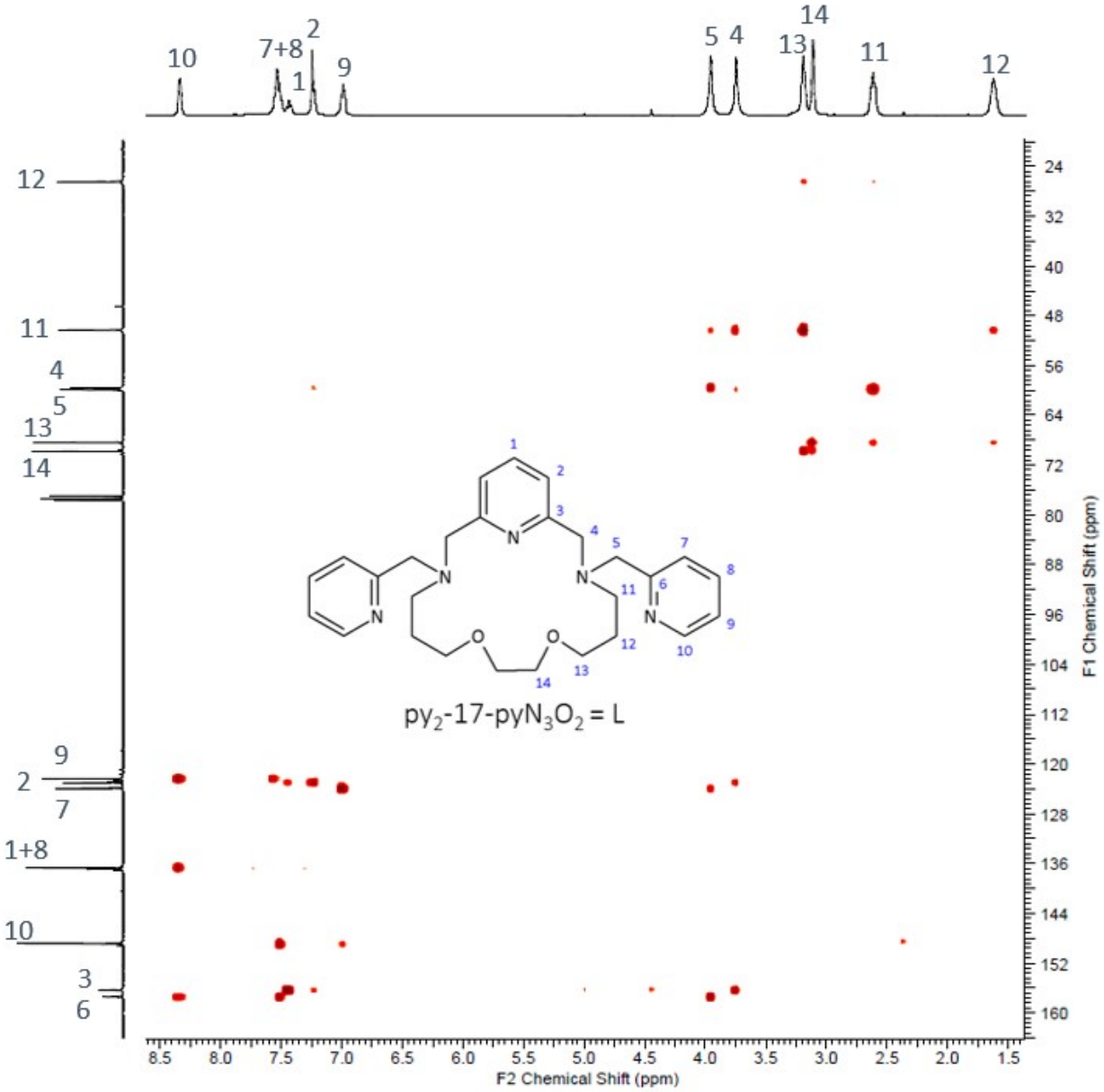

Figure S5: ^{1}H–^{13}C *gs*-HMBC NMR spectrum (400 MHz, $CDCl_3$) of **L** (3,14-bis(2-methylpyridine)-3,14,20-triaza-7,10-dioxabicyclo[14.3.1]dodeca-1(20),16,18-triene) with a residual peak of $CHCl_3$ at 7.27 ppm (^{1}H) and $CDCl_3$ at 77.0 ppm (^{13}C).

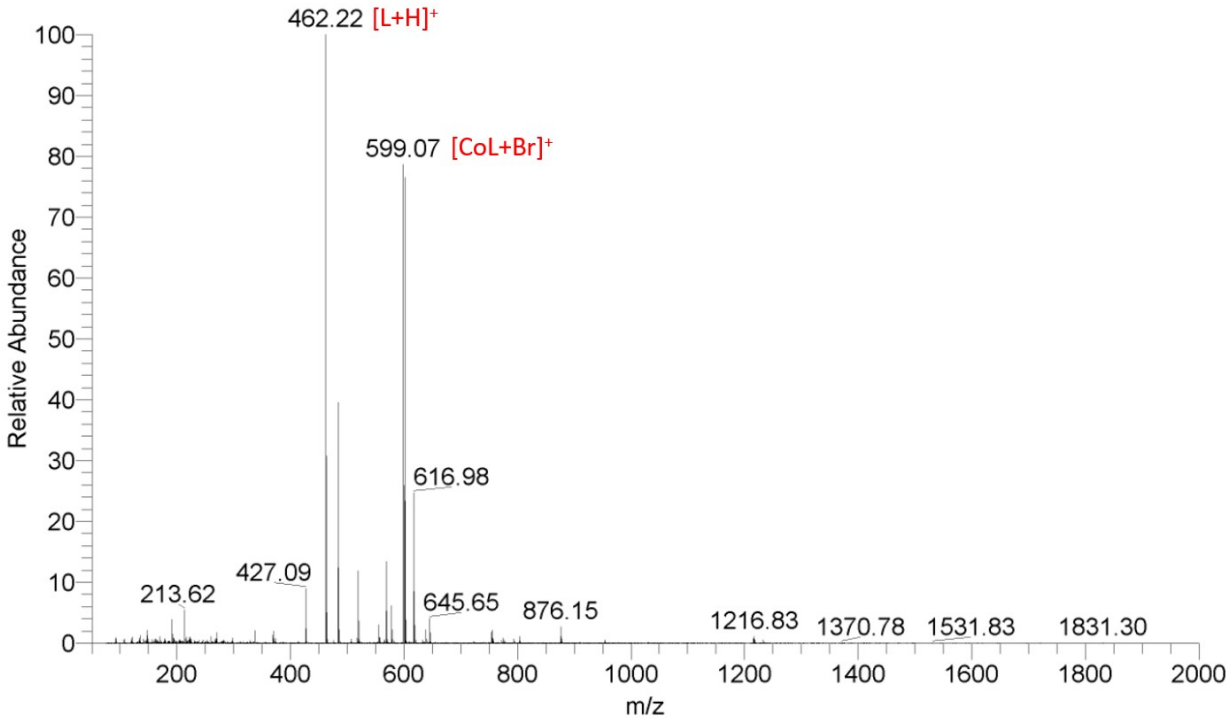

Figure S6 ESI-MS spectrum of complex **1** in positive mode.

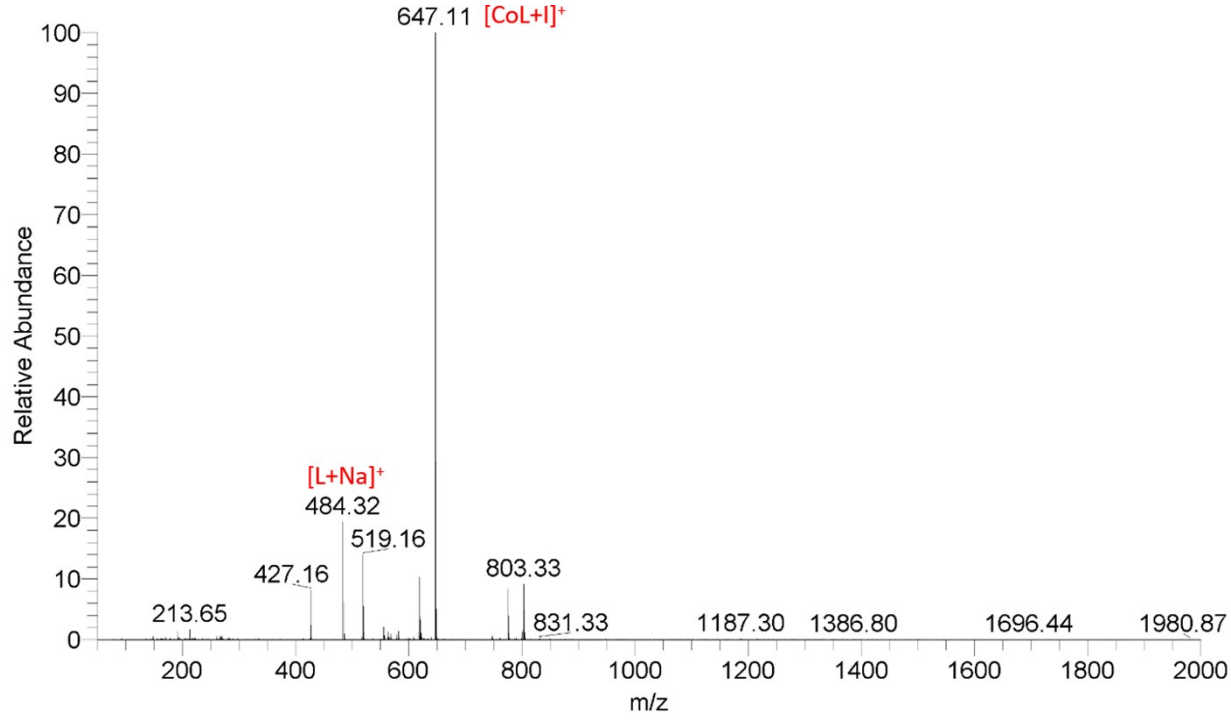

Figure S7 ESI-MS spectrum of complex **2** in positive mode.

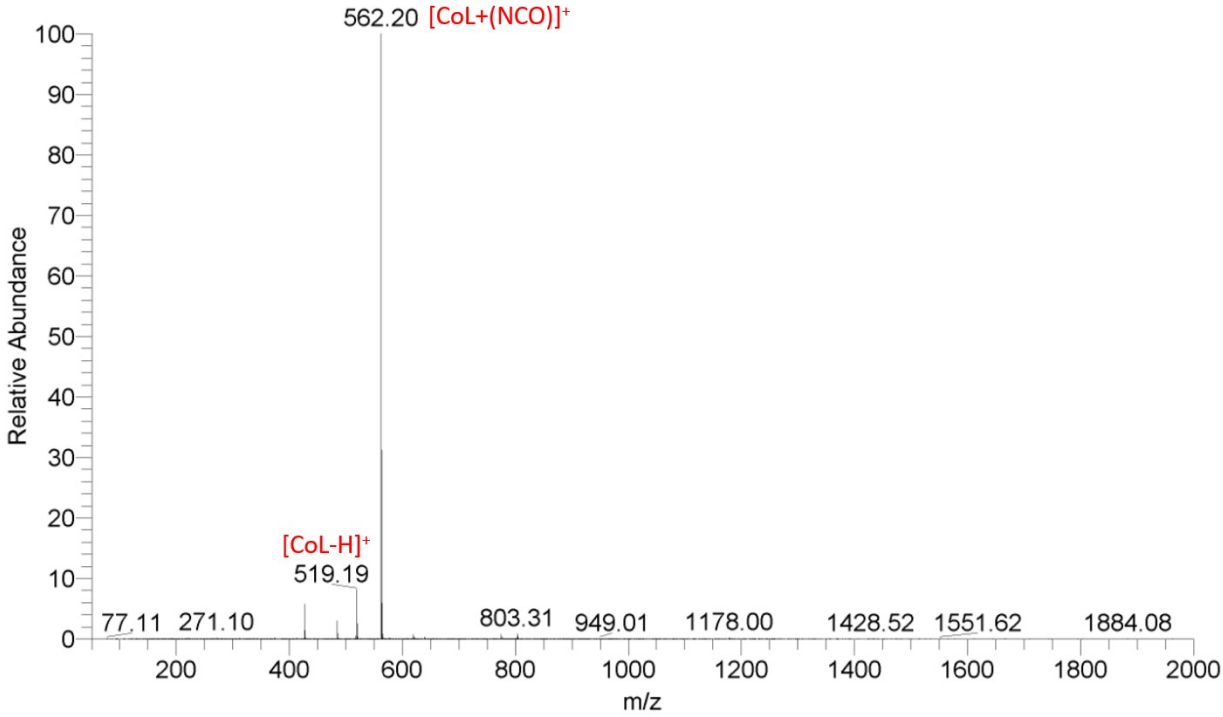

Figure S8 ESI-MS spectrum of complex **3** in positive mode.

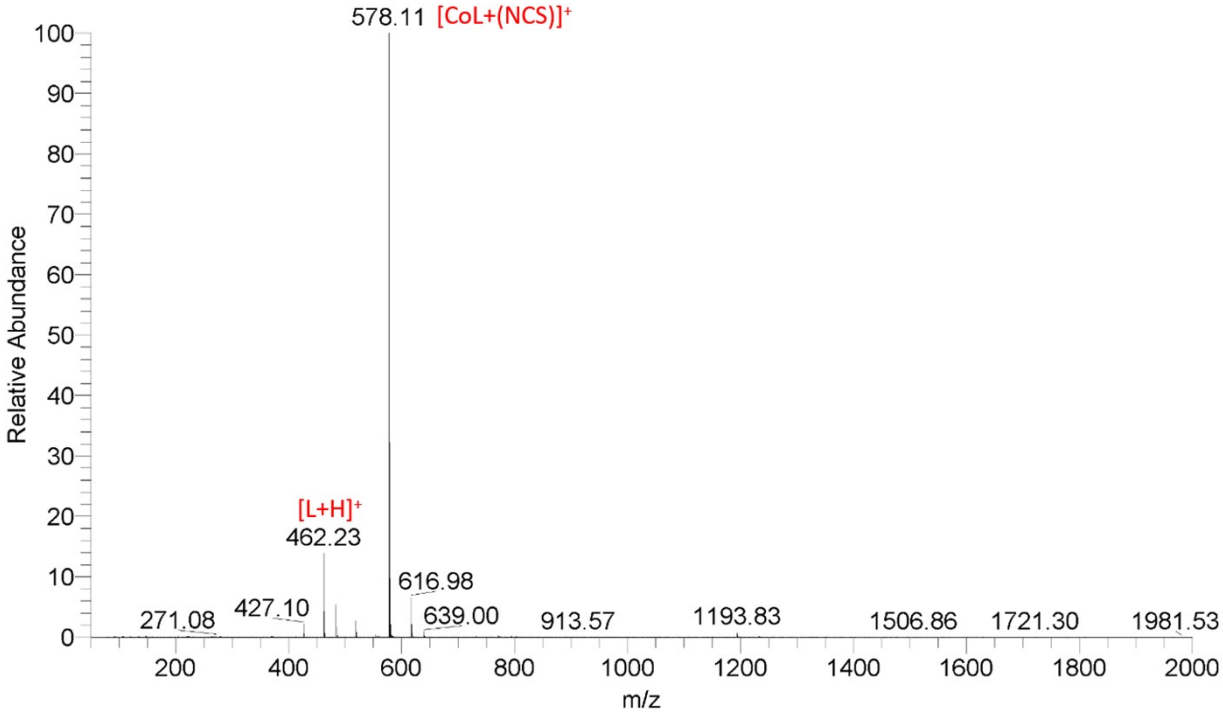

Figure S9 ESI-MS spectrum of complex **4a** in positive mode.

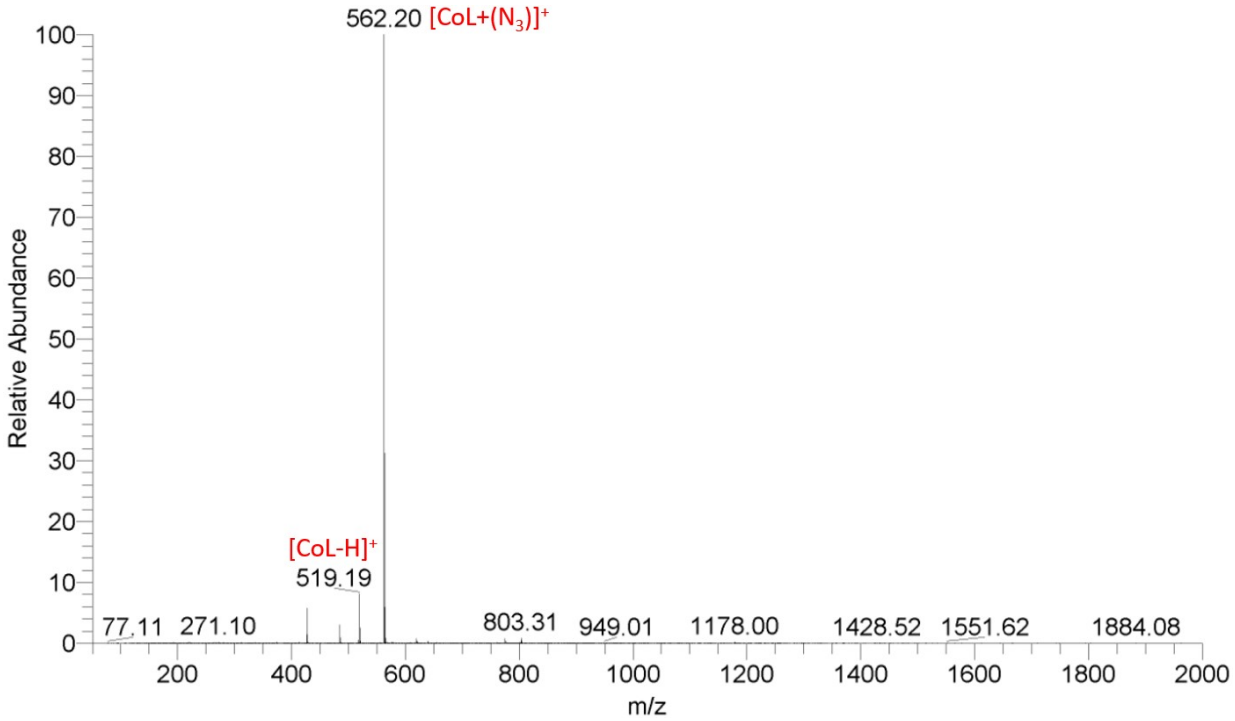

Figure S10 ESI-MS spectrum of complex **5** in positive mode.

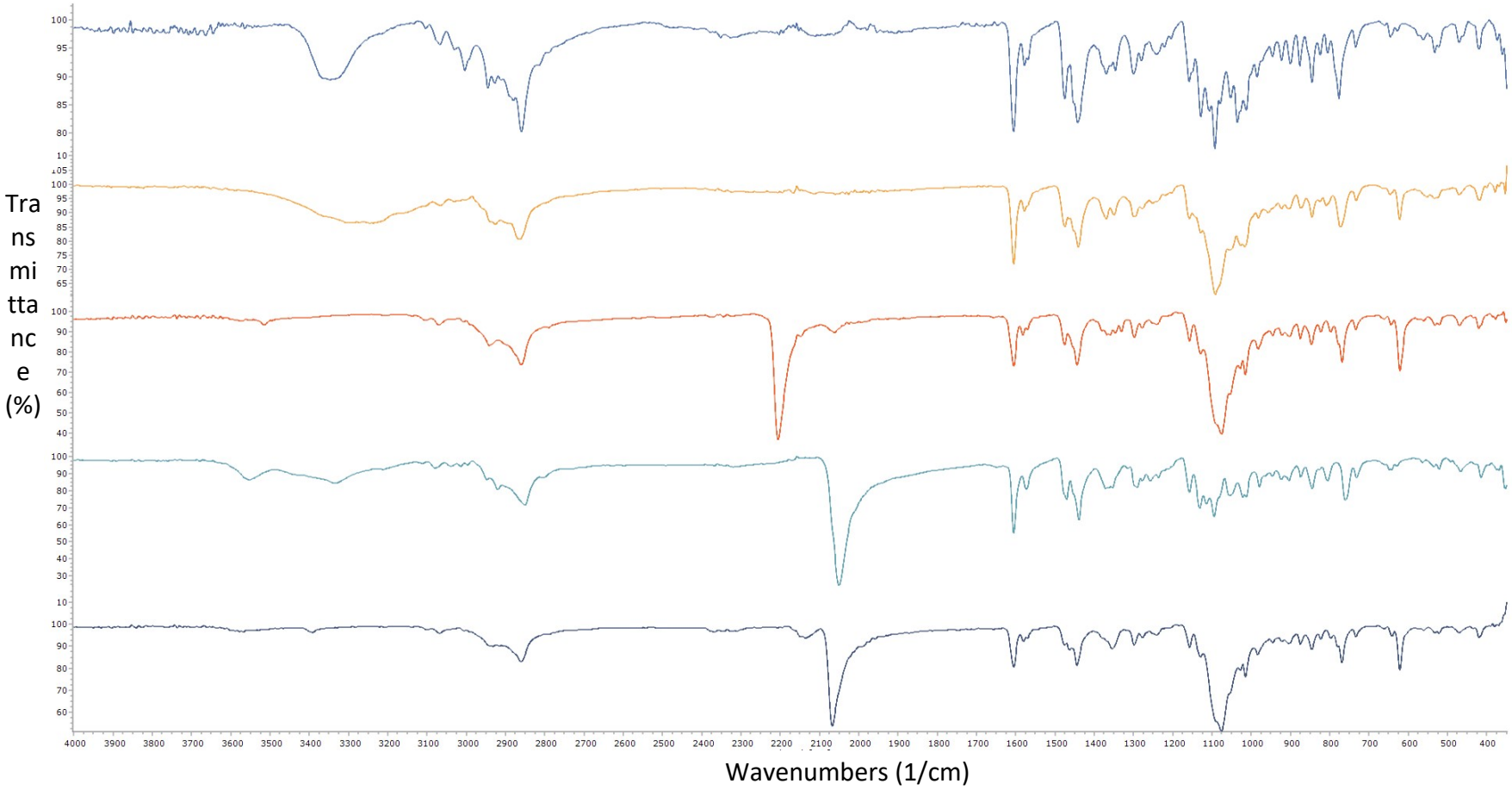

Figure S11 Comparison of IR spectra of studied complexes **1**–**5**. Curve colours: blue = **1**; yellow = **2**; red = **3**; green = **4a**; grey = **5**.

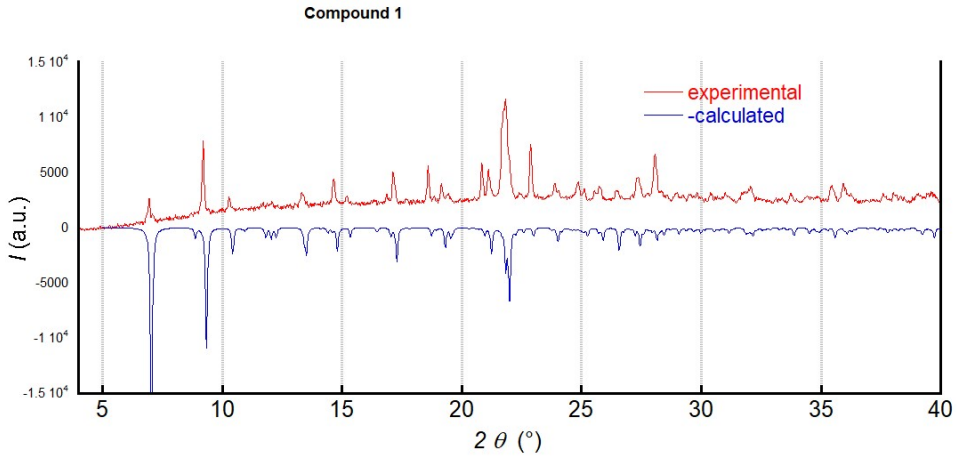
Compound 1
experimental
-calculated
I (a.u.)
2 θ (°)

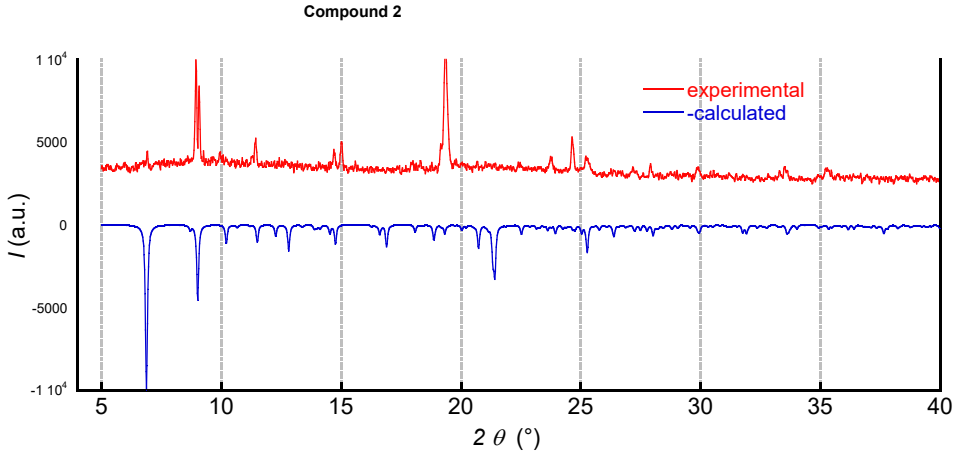
Compound 2
experimental
-calculated
I (a.u.)
2 θ (°)

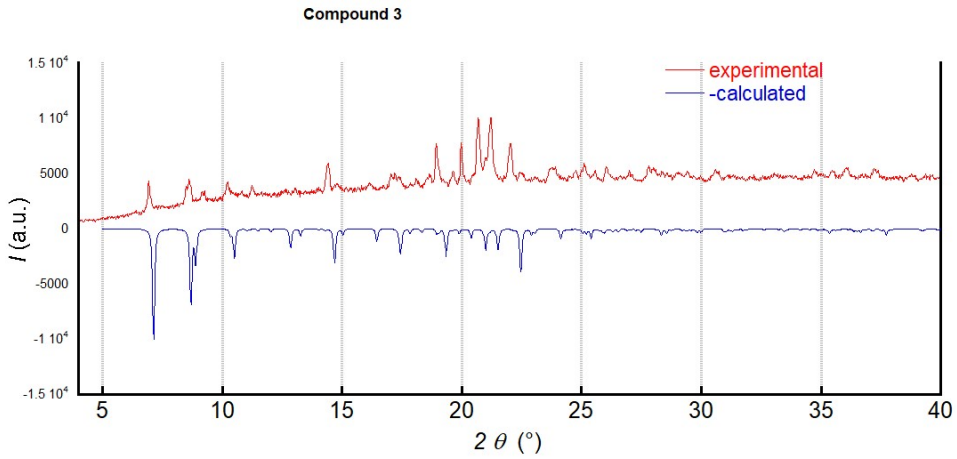
Compound 3
experimental
-calculated
I (a.u.)
2 θ (°)

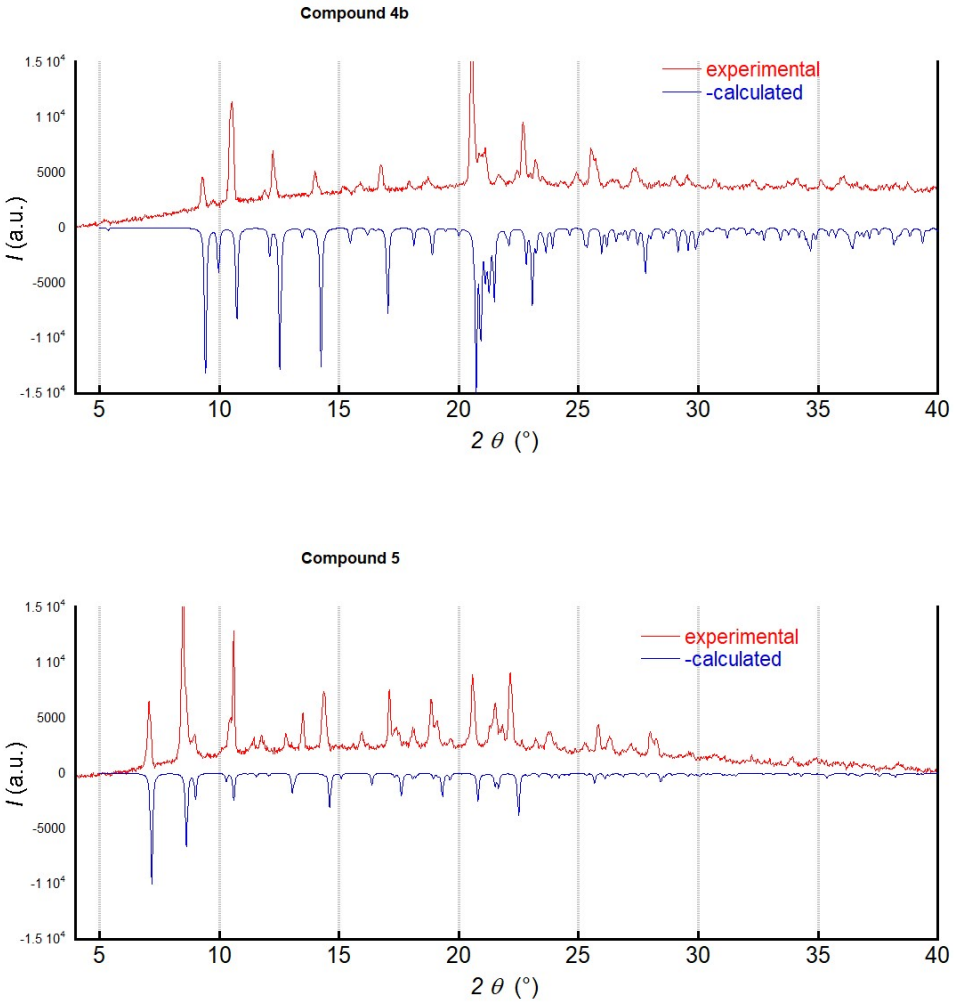

Figure S12 The X-ray powder diffraction patterns for complexes **1**–**5** compared to those calculated from single-crystal X-ray analysis.

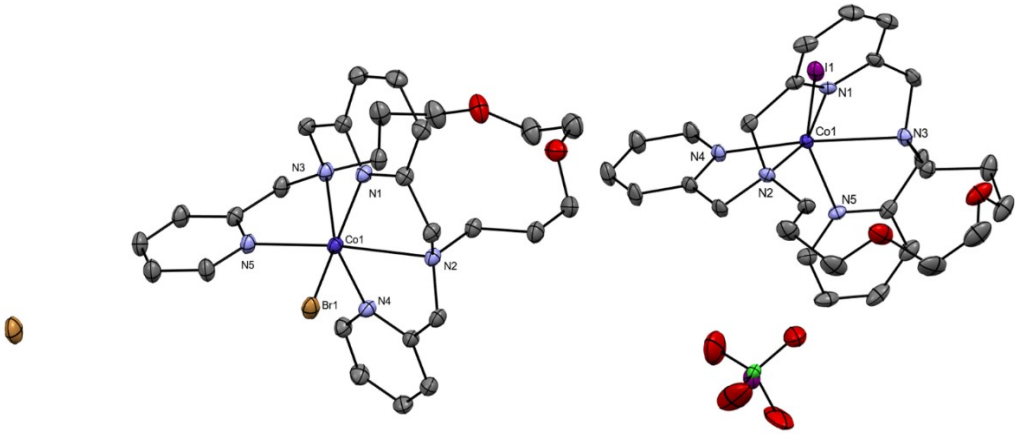

Figure S13 The molecular structures of the complexes **1** (*left*) and **2** (*right*). Atoms are drawn as thermal ellipsoids at the 15% probability level. Hydrogen atoms were omitted for clarity.

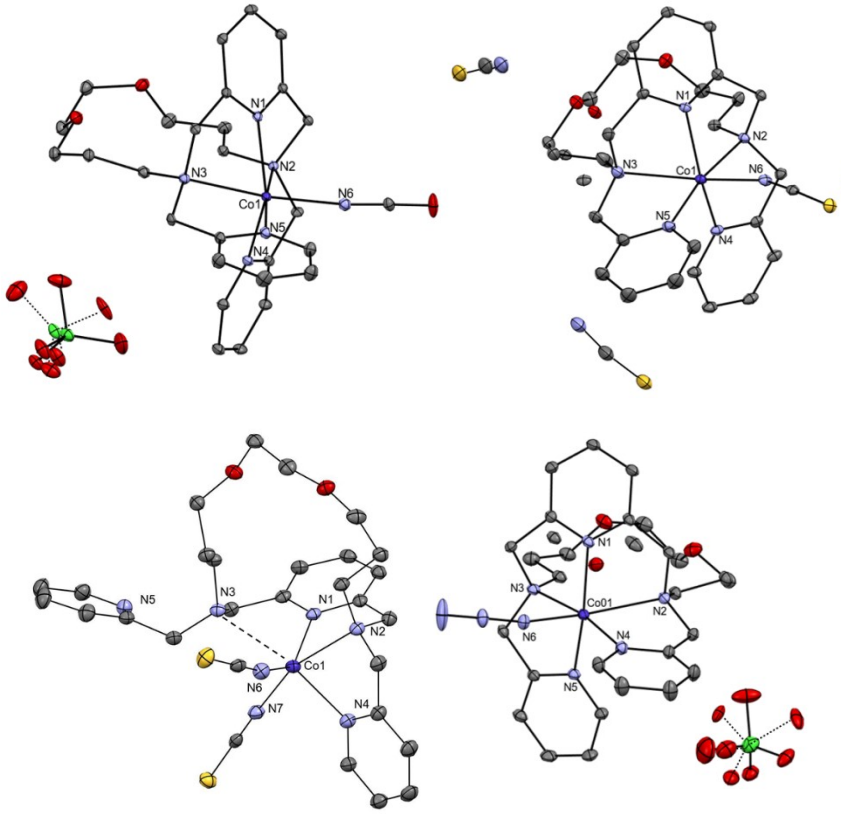

Figure S14 The molecular structures of the complexes **3, 4a, 4b and 5** (from *left* to *right* and *top* to *bottom*). Atoms are drawn as thermal ellipsoids at the 15% probability level. Hydrogen atoms were omitted for clarity.

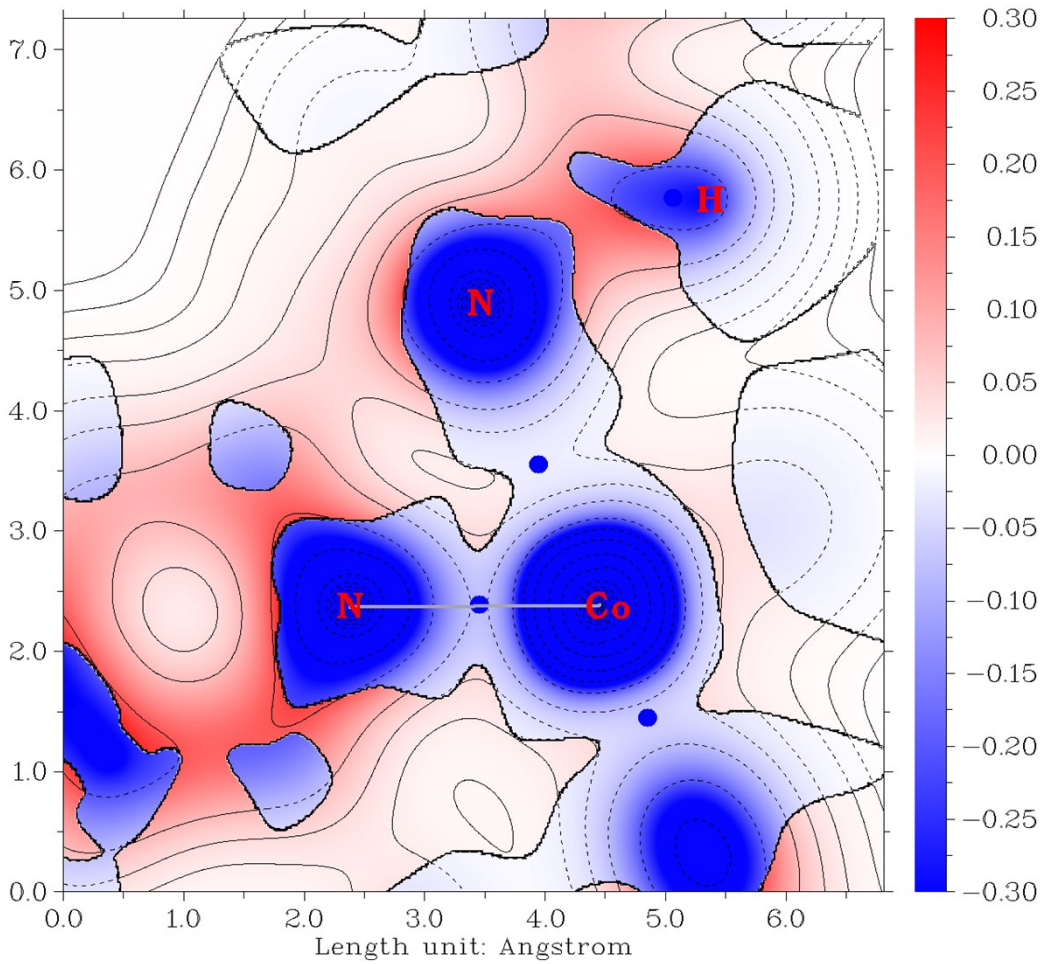

Figure S15 Sign(λ_2)ρ plot of complex **4b** in the vicinity of Co1···N3. Bond critical points of type (3,-1) are represented as blue dots.

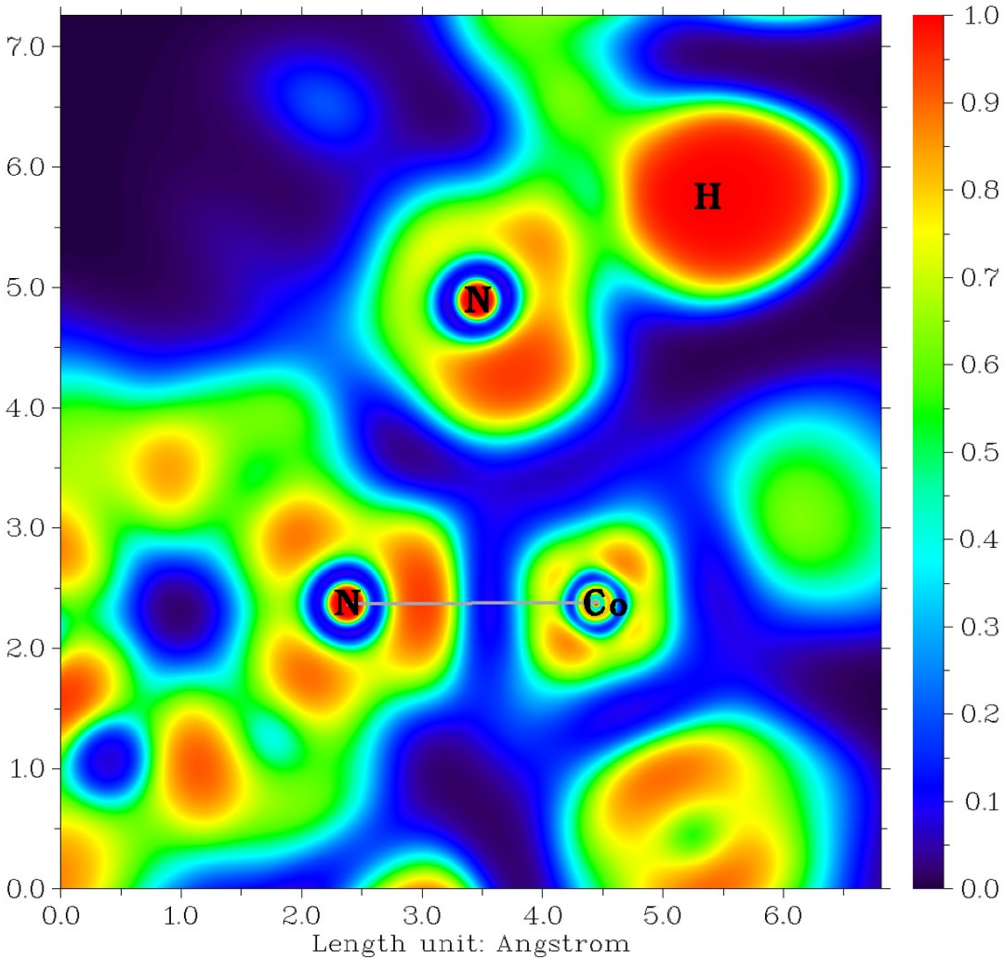

Figure S16 Electron localization function plot of complex **4b** in the vicinity of Co1···N3.

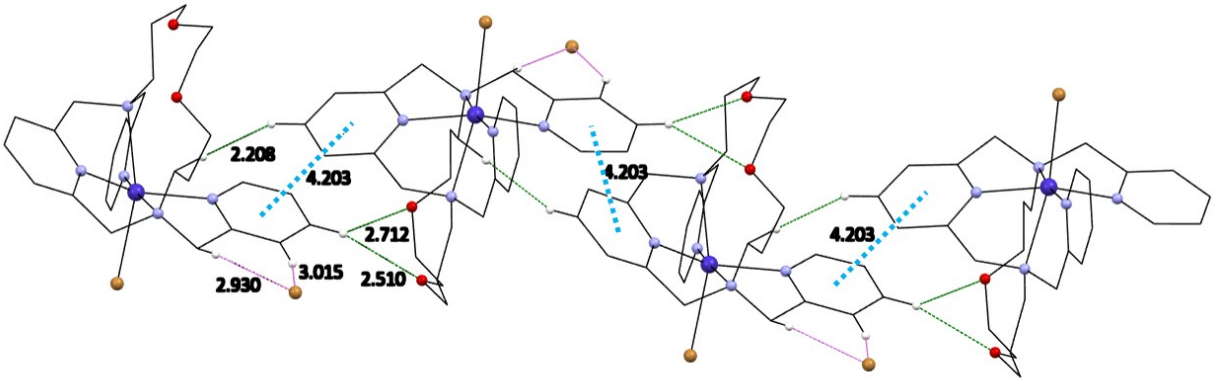

Figure S17 Visualization of π-π stacking interactions with centroids distances (blue dashed lines) between two pyridine rings and hydrogen bonds distances (green lines) for complex **1**.

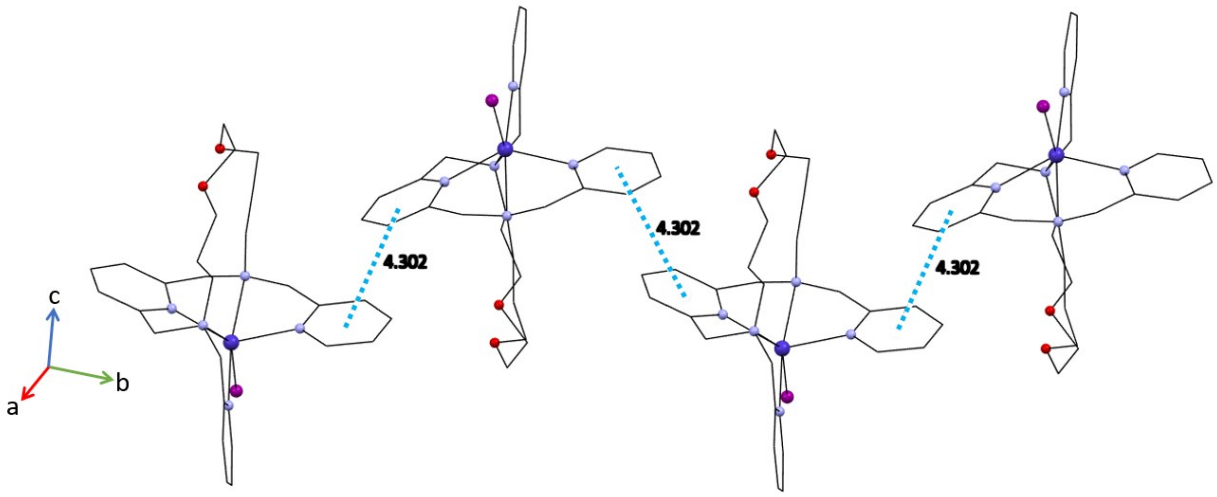

Figure S18 Visualization of π-π stacking interactions with centroids distances (blue dashed lines) between two pyridine rings for complex **2**.

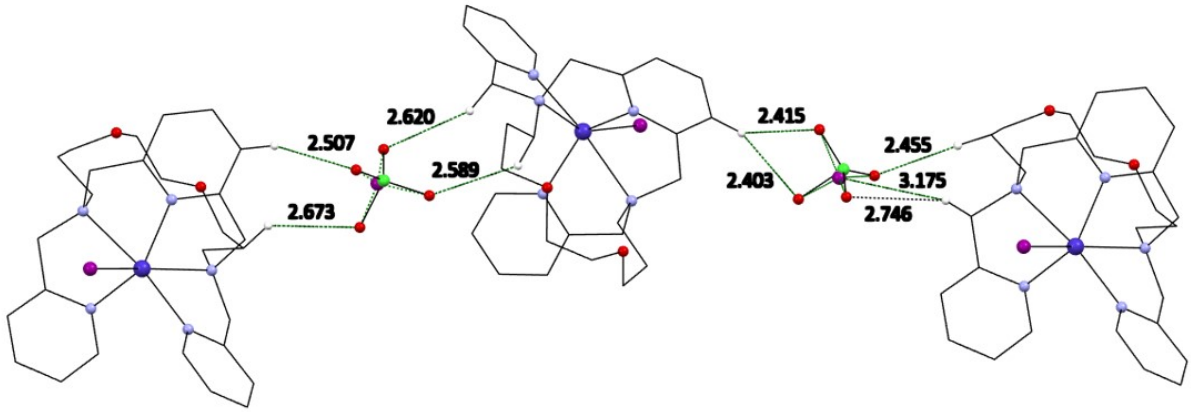

Figure S19 Visualization of half of the uncoordinated perchlorate anions substituted by iodide anions including hydrogen bonds distances for complex **2**.

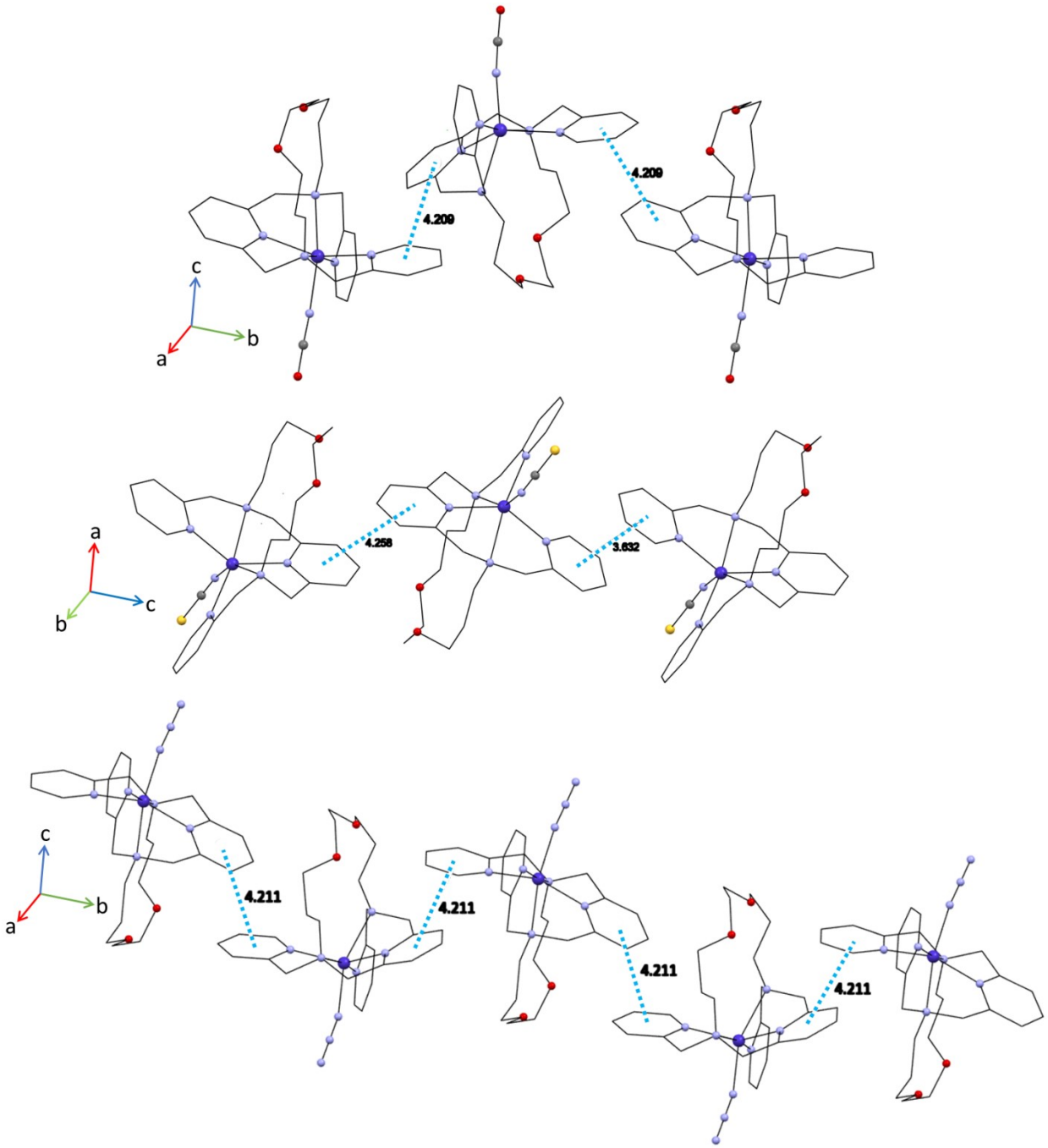

Figure S20 Visualization of π-π stacking interactions with centroids distances (blue dashed lines) between two pyridine rings for complexes **3**–**5** from top to bottom.

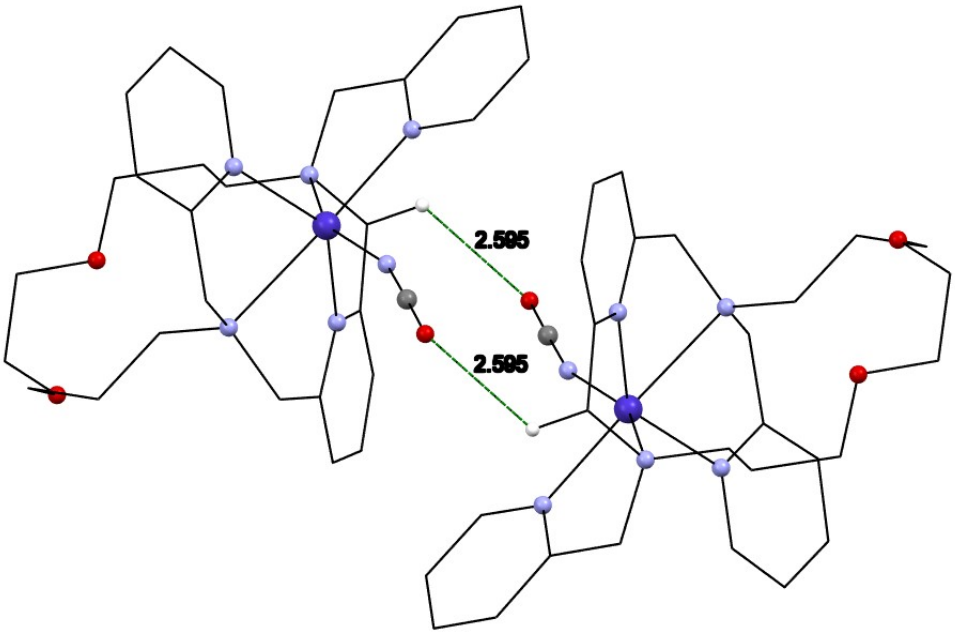

Figure S21 The molecules of complex **3** oriented in antiparallel directions and formation of supramolecular dimer via hydrogen bonds between the NCO^- aliphatic $–CH_2–$ groups bearing pyridine rings with displayed bond distances.

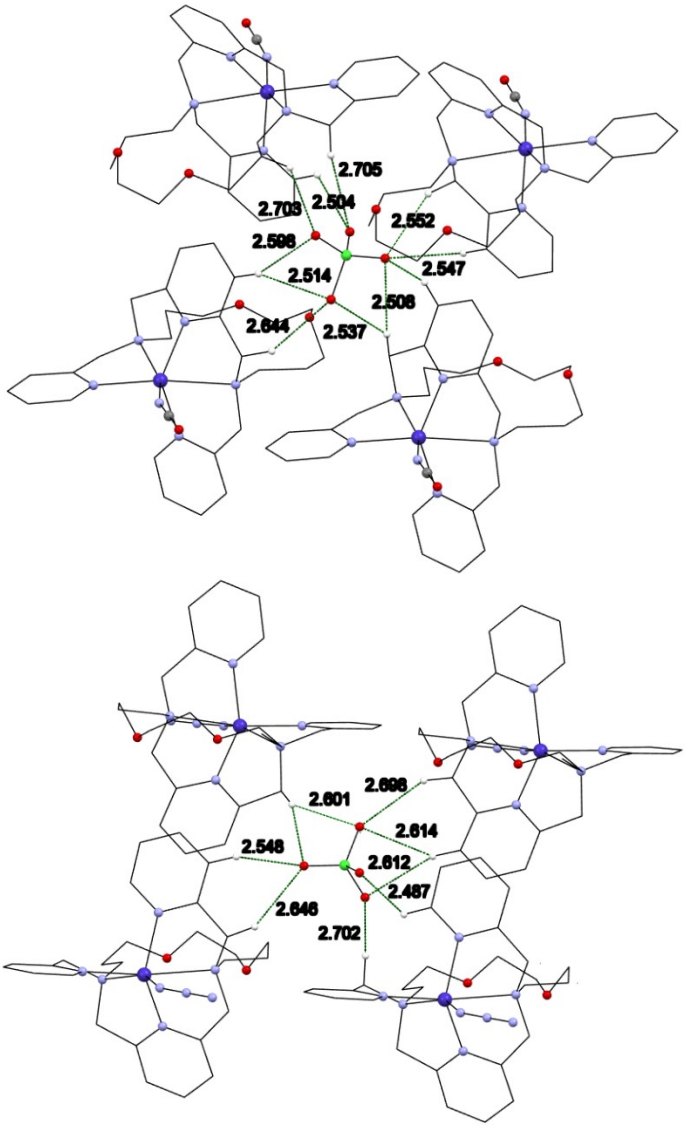

Figure S22 Supramolecular 3D network formed via C_{arom}–H···O–Cl–O···H–C_{arom} hydrogen bonds for complexes **3** (*top*) and **5** (*bottom*).

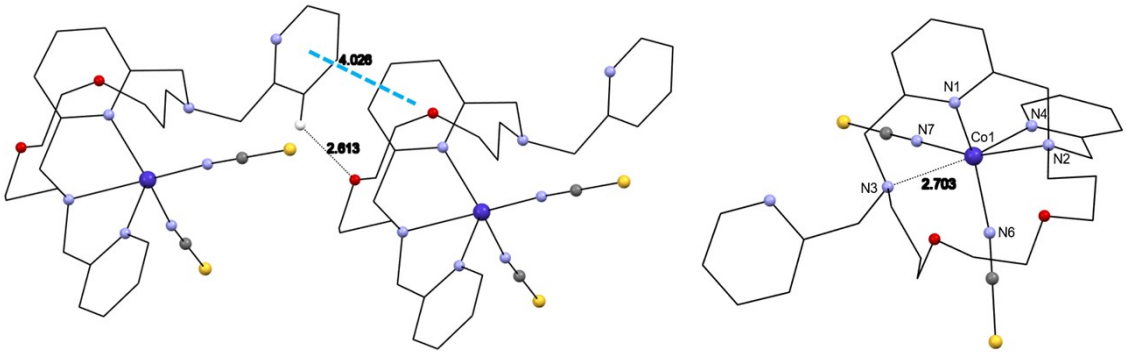

Figure S23 Visualization of π-π stacking interactions with centroids distances (blue dashed lines) between two pyridine rings and hydrogen bonds distances (green lines) for complex **4b**.

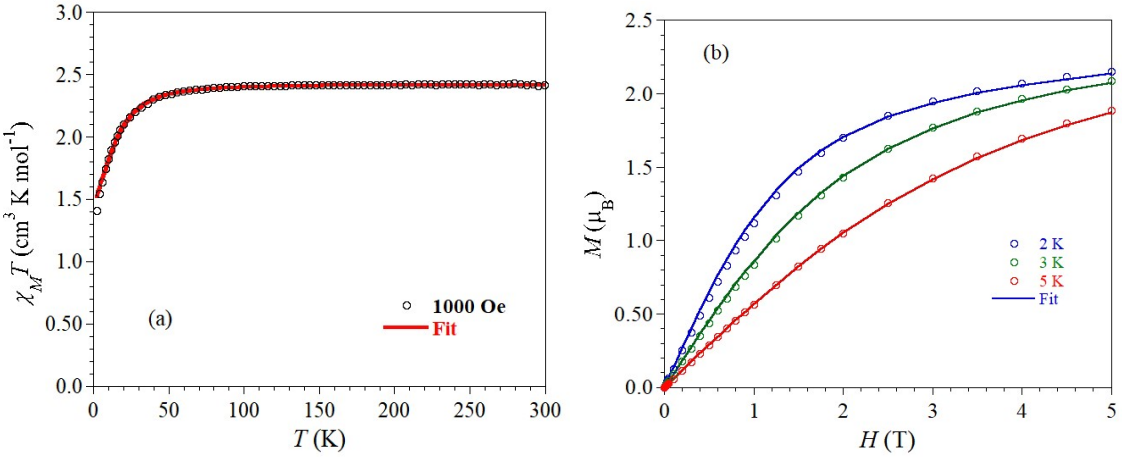

Figure S24 Complex **1**: (a) Temperature dependence of $\chi_M T$ at 1000 Oe and (b) field dependence of magnetization at 2, 3 and 5 K under magnetic fields up to 5 T. The lines materialize the best fit (see text).

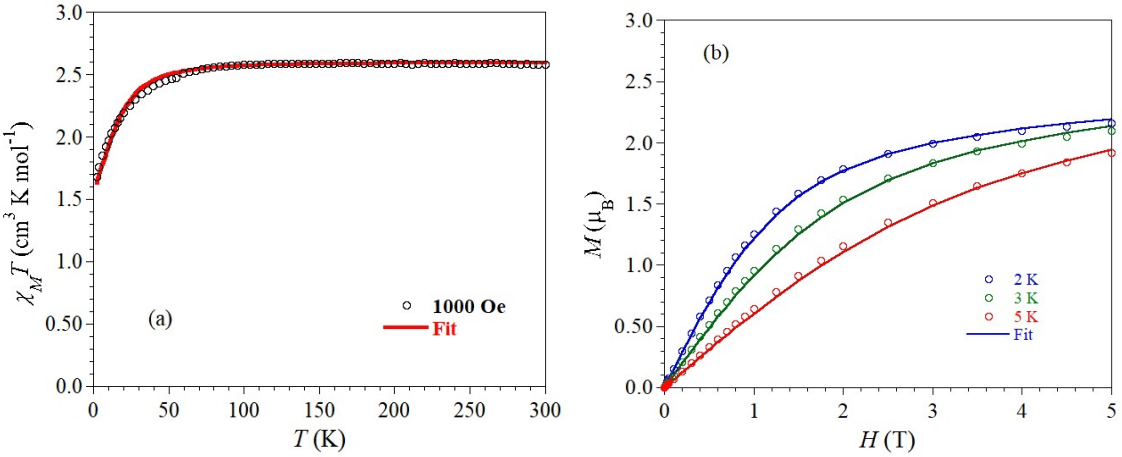

Figure S25 Complex **2**: (a) Temperature dependence of $\chi_M T$ at 1000 Oe and (b) field dependence of magnetization at 2, 3 and 5 K under magnetic fields up to 5 T. The lines materialize the best fit (see text).

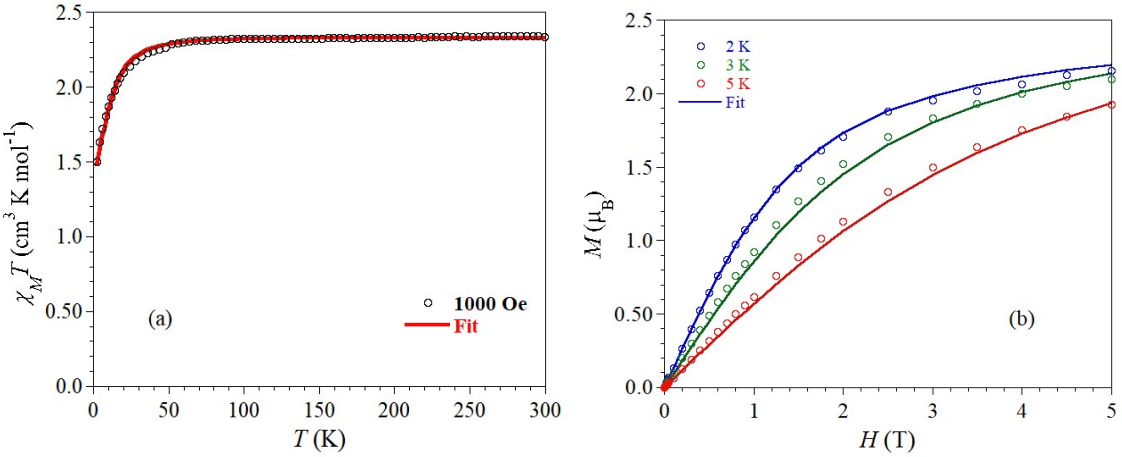

Figure S26 Complex **3**: (a) Temperature dependence of $\chi_M T$ at 1000 Oe and (b) field dependence of magnetization at 2, 3 and 5 K under magnetic fields up to 5 T. The lines materialize the best fit (see text).

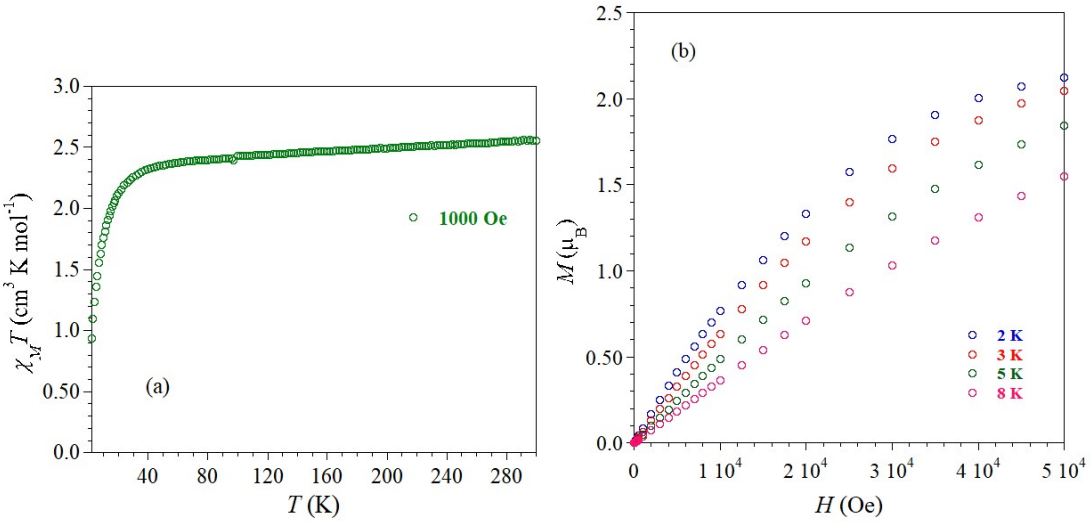

Figure S27 Complex **5**: (a) Temperature dependence of $\chi_M T$ at 1000 Oe and (b) field dependence of magnetization at 2, 3 and 5 K under magnetic fields up to 5 T.

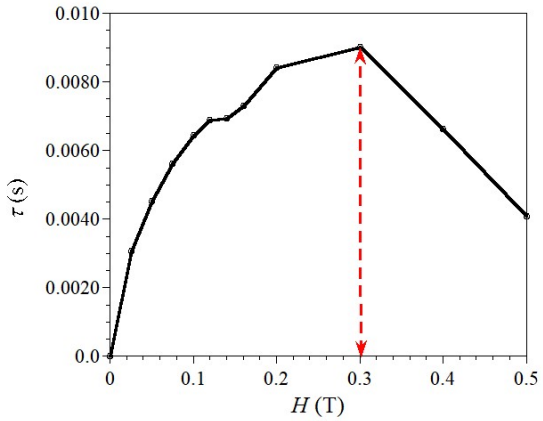

Figure S28 Complex **4b:** Field dependence of the out-of-phase component of the ac signal measured at 2 K.

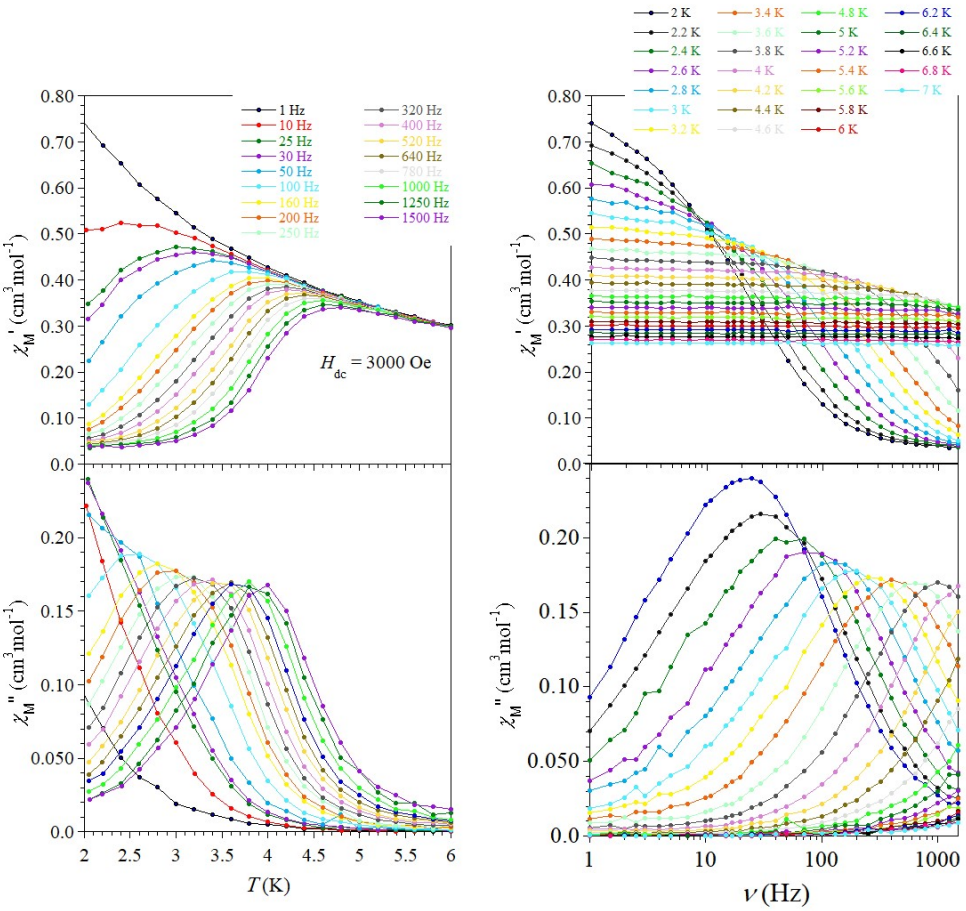

Figure S29 Complex **4b**: Temperature and field dependence of the in-phase and out-of-phase component of the ac signal under a dc magnetic field of 3 kOe.

Table S1 Selected bond angles for complexes **1**–**5**, where X stands for Br (**1**), I (**2**), NCO (**3**), NCS (**4a**) and N_3 (**5**) respectively. The three largest values are given in red color.

Complex	**1**	**2**	**3**	**4a**	**5**		**4b**
Atoms	Angle (°)					Atoms	
N1–Co1–N2	70.1(1)	73.0(1)	70.0(1)	72.1(1)	74.1(1)	N1–Co1–N2	74.58(6)
N1–Co1–N3	73.0(1)	70.6(1)	73.8(1)	73.3(1)	70.6(1)	N1–Co1–N4	112.35(6)
N1–Co1–N4	137.6(1)	117.4(2)	136.8(1)	140.0(1)	118.4(1)	N2–Co1–N4	73.81(6)
N1–Co1–N5	116.0(1)	138.9(1)	116.8(1)	116.0(1)	137.8(1)	N1–Co1–N6	138.80(7)
N2–Co1–N3	110.4(1)	111.5(1)	113.1(1)	114.9(1)	114.0(1)	N2–Co1–N6	89.92(6)
N2–Co1–N4	73.5(1)	72.7(1)	73.3(1)	74.1(1)	73.0(1)	N4–Co1–N6	98.87(7)
N2–Co1–N5	173.9(1)	103.3(1)	172.6(1)	171.1(1)	101.6(1)	N1–Co1–N7	100.97(6)
N3–Co1–N4	100.6(1)	172.0(2)	101.3(1)	102.9(1)	170.5(1)	N2–Co1–N7	158.75(6)
N3–Co1–N5	72.2(1)	73.3(1)	72.8(1)	72.3(1)	73.6(1)	N4–Co1–N7	89.36(7)
N4–Co1–N5	100.6(2)	99.3(2)	101.5(1)	99.5(1)	99.2(1)	N6–Co1–N7	105.73(7)
X–Co1–N1	102.5(1)	100.4(1)	101.8(1)	99.0(1)	102.2(1)	N3–Co1–N6	85.81(6)
X–Co1–N2	87.32(9)	155.41(9)	85.4(1)	84.7(1)	153.4(1)	N3–Co1–N7	79.75(6)
X–Co1–N3	158.0(1)	87.4(1)	157.0(1)	154.2(1)	88.4(1)	N3–Co1–N1	68.64(5)
X–Co1–N4	96.9(1)	90.7(1)	97.0(1)	98.6(1)	86.6(1)	N3–Co1–N2	116.37(5)
X–Co1–N5	91.6(1)	97.1(1)	90.1(1)	90.2(1)	98.3(1)	N3–Co1–N4	168.98(6)

Table S2 Continuous shape measurement for complexes **1**–**5**. (HP-6 = Hexagon; PPY-6 = Pentagonal pyramid; OC-6 = Octahedron; TPR-6 = Trigonal prism; JPPY-6 = Johnson pentagonal pyramid). The smallest deviation from the optimal shape is highlighted in blue filling.

Complex	**1**	**2**	**3**	**4a**	**4b**	**5**
HP-6	28.413	29.006	27.748	27.646	27.723	28.324
PPY-6	13.981	14.498	13.457	13.868	12.418	13.338
OC-6	6.734	7.389	7.003	6.934	7.219	7.316
TPR-6	8.748	8.829	7.724	7.141	7.366	7.151
JPPY-6	16.749	17.219	16.611	17.090	15.360	16.498

Table S3 Calculated individual non-zero contributions to *D*-tensor for studied complexes **1**–**5** obtained from the CASSCF/NEVPT2 calculations.

Complex 1 (Br^{-})

Multiplicity	Root	D	E
4	1	-19.732	-3.506
4	2	-1.355	-6.786
4	3	-2.918	-0.883
4	4	6.571	5.749
4	5	0.167	-0.008
4	6	0.019	-0.024
4	7	0.01	-0.015
4	8	-0.021	0
4	9	0.001	-0.002
2	0	-0.416	1.16
2	1	-0.688	-0.665
2	2	0	-0.003
2	3	0.196	-0.019
2	4	0.023	-0.003
2	5	0.068	-0.001
2	6	2.205	0.378
2	7	-0.658	1.273
2	8	-2.207	-2.147
2	9	0.397	0.21
2	10	0.195	0.024
2	11	-0.029	0.026
2	12	0.025	0.026
2	13	0.045	0.239
2	14	-0.061	-0.036
2	15	0.203	0.051
2	16	-0.181	0.187
2	17	0.088	-0.013
2	18	-0.096	-0.095
2	19	-0.057	0.015
2	20	-0.319	-0.344
2	21	-0.339	-0.408
2	22	-0.048	-0.051
2	23	-0.387	0.384
2	24	0.073	0.035
2	25	0.456	0.016
2	26	0.004	-0.001
2	27	-0.014	-0.007
2	28	-0.004	0.003
2	29	0.121	-0.035

2	30	-0.099	0.096
2	31	0.072	-0.065
2	32	-0.008	0.006
2	33	0.007	0.01
2	34	0.001	0
2	35	-0.001	0.005
2	36	0	-0.008
2	37	-0.004	-0.002
2	38	-0.008	-0.006
2	39	-0.017	0.013

Complex 2 (I^-)

Multiplicity	**Root**	**D**	**E**
4	1	-30.42	-1.375
4	2	3.372	-7.428
4	3	-1.295	-1.253
4	4	4.251	4.326
4	5	0.68	0.074
4	6	0.017	-0.014
4	7	0.006	-0.007
4	8	-0.013	0
4	9	-0.005	0
2	0	-0.704	0.356
2	1	-0.417	-0.438
2	2	0.042	-0.002
2	3	0.097	-0.012
2	4	0.147	-0.014
2	5	0.106	0.01
2	6	2.922	0.03
2	7	-1.48	1.22
2	8	-2.22	-2.016
2	9	0.37	0.183
2	10	0.116	0.028
2	11	-0.075	0.081
2	12	0.023	-0.007
2	13	0.086	0.153
2	14	-0.093	0.042
2	15	0.252	0.001
2	16	-0.242	0.209
2	17	0.033	-0.024
2	18	-0.095	-0.07
2	19	-0.133	-0.066

2	20	-0.278	-0.249
2	21	-0.309	-0.432
2	22	-0.042	-0.035
2	23	-0.383	0.393
2	24	0.123	-0.013
2	25	0.34	0.024
2	26	0.006	-0.001
2	27	-0.006	0.005
2	28	-0.01	0.001
2	29	0.076	-0.043
2	30	-0.086	0.082
2	31	0.102	-0.037
2	32	-0.014	0.012
2	33	0.006	0.012
2	34	0.001	0
2	35	0	0.005
2	36	-0.003	-0.007
2	37	-0.002	0
2	38	-0.007	-0.009
2	39	-0.025	0

Complex 3 (NCO^-)

Multiplicity	**Root**	**D**	**E**
4	1	-29.79	-1.499
4	2	5.914	-7.547
4	3	1.716	0.124
4	4	5.683	4.623
4	5	0.196	-0.318
4	6	-0.001	-0.003
4	7	-0.024	0.004
4	8	0.037	-0.03
4	9	-0.036	0.001
2	0	0.449	-0.381
2	1	0.726	0.343
2	2	0.109	0.005
2	3	0.097	-0.005
2	4	0.476	0.001
2	5	0.523	0.25
2	6	2.056	0.06
2	7	-1.043	1.347
2	8	-2.073	-1.929

2	9	-0.2	0.193
2	10	-0.007	0.028
2	11	0.249	0.057
2	12	-0.11	0.182
2	13	0.631	0.028
2	14	-0.065	0.091
2	15	-0.012	-0.043
2	16	-0.155	0.098
2	17	0.187	0
2	18	-0.032	-0.036
2	19	0.317	0.029
2	20	-0.721	-0.705
2	21	-0.179	0.003
2	22	-0.342	0.342
2	23	0.02	-0.02
2	24	0.023	0.043
2	25	0.331	0.035
2	26	-0.001	-0.002
2	27	-0.009	-0.01
2	28	-0.04	-0.006
2	29	0.061	0.01
2	30	0.032	-0.075
2	31	-0.057	0.07
2	32	0.017	-0.001
2	33	-0.008	0.008
2	34	-0.001	0.001
2	35	0.016	0.004
2	36	-0.012	0.005
2	37	-0.008	-0.002
2	38	0.039	0.004
2	39	-0.016	-0.011

Complex 4a (NCS^-)

Multiplicity	**Root**	**D**	**E**
4	1	-31.293	-1.774
4	2	5.376	-7.889
4	3	-0.863	-1.786
4	4	6.122	6.396
4	5	0.277	-0.277
4	6	0.015	-0.025
4	7	0.002	-0.021
4	8	-0.015	-0.013
4	9	-0.013	-0.001

2	0	1.169	0.666
2	1	-0.701	-0.316
2	2	0.007	-0.006
2	3	0.204	-0.012
2	4	0.381	0.003
2	5	0.085	0.018
2	6	2.489	0.249
2	7	-1.023	1.358
2	8	-2.028	-2.053
2	9	-0.175	0.372
2	10	0.361	0.002
2	11	0.032	0.006
2	12	-0.025	0.046
2	13	0.405	0.129
2	14	0.04	0.101
2	15	-0.073	0.007
2	16	-0.054	0.107
2	17	0.126	0.009
2	18	-0.041	0.006
2	19	0.173	0.104
2	20	-0.731	-0.851
2	21	-0.264	0.139
2	22	-0.239	0.217
2	23	0.015	-0.019
2	24	0.017	0.054
2	25	0.338	0.011
2	26	-0.001	-0.003
2	27	-0.01	-0.01
2	28	0.023	0.009
2	29	0.071	0.002
2	30	0.065	-0.028
2	31	-0.105	0.015
2	32	0.011	0.004
2	33	-0.011	0.018
2	34	0	0.001
2	35	0.006	0.004
2	36	-0.015	-0.006
2	37	-0.006	-0.007
2	38	0.026	0.015
2	39	-0.007	-0.004

Complex 4b (NCS^-)

Multiplicity	**Root**	**D**	**E**
4	1	-27.584	-2.097
4	2	4.723	-8.002

4	3	-1.589	-1.325
4	4	6.892	6.197
4	5	-0.423	-0.344
4	6	0.071	0.054
4	7	-0.002	0.003
4	8	0.032	0.014
4	9	-0.021	-0.008
2	0	-0.466	-0.604
2	1	-0.08	0.57
2	2	0.158	0.003
2	3	0.01	-0.001
2	4	0.418	0.077
2	5	-0.022	0.064
2	6	2.84	0.011
2	7	-1.192	1.144
2	8	-1.833	-1.279
2	9	-0.266	0.26
2	10	0.451	0.066
2	11	0.001	0
2	12	0.221	0.05
2	13	0.117	0.017
2	14	0.213	0.125
2	15	-0.005	-0.008
2	16	-0.122	0.084
2	17	-0.012	-0.076
2	18	0.119	0.014
2	19	-0.077	-0.131
2	20	-0.802	-0.585
2	21	-0.065	-0.059
2	22	-0.374	0.293
2	23	-0.04	-0.044
2	24	0.041	0.014
2	25	0.376	0.011
2	26	-0.002	0.001
2	27	-0.006	-0.005
2	28	0.101	0.014
2	29	0.13	-0.016
2	30	-0.096	-0.056
2	31	-0.07	0.04
2	32	0.018	0.004
2	33	-0.002	0.013
2	34	0.001	0
2	35	-0.004	0.008
2	36	-0.009	0.006
2	37	-0.001	0

2	38	0.005	-0.002
2	39	-0.001	-0.01

Complex 5 (N_3^-)

Multiplicity	**Root**	**D**	**E**
4	1	-26.488	-2.068
4	2	4.418	-7.103
4	3	3.782	4.571
4	4	2.058	0.594
4	5	0.086	-0.181
4	6	0.022	-0.03
4	7	0.004	-0.016
4	8	-0.009	-0.013
4	9	-0.019	-0.001
2	0	0.358	-0.056
2	1	-0.124	0.391
2	2	0.066	-0.01
2	3	0.21	-0.014
2	4	0.339	-0.003
2	5	-0.031	0.108
2	6	2.445	0.29
2	7	-0.816	1.305
2	8	-2.167	-2.098
2	9	-0.253	0.289
2	10	0.106	0.013
2	11	0.439	0.012
2	12	0.095	0.063
2	13	0.255	0.158
2	14	-0.038	0.119
2	15	-0.009	-0.056
2	16	-0.133	0.099
2	17	0.165	-0.002
2	18	-0.057	-0.062
2	19	0.195	0.08
2	20	-0.598	-0.661
2	21	-0.108	-0.107
2	22	-0.464	0.452
2	23	-0.024	-0.038
2	24	0.049	0.051
2	25	0.376	0.017
2	26	0	-0.002
2	27	-0.008	-0.01
2	28	-0.011	-0.025
2	29	0.087	-0.001

2	30	0.079	-0.065
2	31	-0.099	0.076
2	32	0.005	0.002
2	33	-0.009	0.011
2	34	-0.001	0.001
2	35	0.006	0.006
2	36	-0.012	0.002
2	37	-0.005	-0.007
2	38	0.013	0.016
2	39	-0.002	-0.013